Toward Ligand-Driven Light-Induced Spin Change. Influence of the Configuration of 4-Styrylpyridine (stpy) on the Magnetic Properties of $Fe^{II}(stpy)_4(NCS)_2$ Complexes. Crystal Structures of the Spin-Crossover Species Fe(*trans*-stpy)$_4$(NCS)$_2$ and of the High-Spin Species Fe(*cis*-stpy)$_4$(NCS)$_2$

Cécile Roux,[1a] Jacqueline Zarembowitch,*[,1a] Bernard Gallois,*[,1b] Thierry Granier,[1b] and Renée Claude[1a]

Laboratoire de Chimie Inorganique (CNRS, URA 420), Université de Paris-Sud, 91405 Orsay, France, and Laboratoire de Cristallographie et de Physique Cristalline (CNRS, URA 144), Université de Bordeaux I, 33405 Talence, France

Received August 11, 1993®

A method to obtain ligand-driven light-induced spin changes (LD–LISC) in transition-metal molecular compounds is described. It is based on the utilization of ligands capable of being photochemically modified, such as *cis–trans* photoisomerizable ligands. A prerequisite for the spin conversion to be observed upon ligand photoisomerization is that one at least of the two complexes formed with ligand isomers presents a thermally-induced spin crossover. Two complexes of the type $FeL_4(NCS)_2$ with L = *trans*-stpy (complex **1**) and L = *cis*-stpy (complex **2**), stpy standing for 4-styrylpyridine, are presented. Their syntheses are described. Their X-ray diffraction structures were determined. **1** crystallizes in the orthorhombic space group $Pna2_1$, with $Z = 4$, $a = 32.004(26)$ Å, $b = 15.394(13)$ Å, and $c = 9.842(10)$ Å. **2** crystallizes in the monoclinic space group $P2_1/n$, with $Z = 2$, $a = 13.115(2)$ Å, $b = 12.569(3)$ Å, $c = 14.574(3)$ Å, and $\beta = 91.90(1)°$. In both complexes, the coordination core has the same geometry, with the NCS^- groups in the *trans* position. Variable-temperature magnetic susceptibility measurements show that **1** presents a $S = 2 \leftrightarrow S = 0$ crossover, centered around 108 K, whereas **2** retains the high-spin state down to 4.2 K. So, this pair of compounds do fulfill the spin-state conditions for the LD–LISC effect to be observed. However, the highest temperature at which the experiment might be carried out is about 90 K. For ligand photoisomerization to occur with suitable quantum yields, this temperautre has now to be increased by modifying the complexes chemically.

Introduction

In a number of transition-metal molecular compounds, the metal ion may exhibit an electronic high-spin (HS) state ↔ low-spin (LS) state crossover under the effect of an external perturbation.[2] In most of the studies reported hitherto, this perturbation is a variation of temperature (at constant pressure) or a variation of pressure (at constant temperature). In both cases, the spin change takes place through the thermal population of the HS and LS levels, the energy of these levels depending on pressure. Furthermore, a quantitative light-induced $^1A_1$ (LS) → $^5T_2$ (HS) transformation may be achieved in a number of iron(II) spin-crossover complexes in the solid state, at a temperature much lower than that of the thermal transition ($<\approx 40$ K), by irradiating the sample into the spin-allowed d–d or MLCT absorption bands of the stable LS species.[3] The metastable HS state which forms in these conditions can remain trapped, with a practically infinite lifetime. This effect, which was termed "light-induced excited spin-state trapping", abbreviated as LIESST, is reversible.

The results reported in the present paper constitute the first part of a work we are carrying out with the object to induce a reversible change of the spin state of the transition-metal ion, in a complex, according to a new strategy which consists in *varying the ligand-field strength under the effect of an electromagnetic radiation*. The phenomenon might be observed at relatively high temperature, indeed even *at room temperature*. The process is based on the utilization of ligands capable of taking part in photoreactions, such as *cis–trans* photoisomerizable ligands. We shall see hereafter that, as a prerequisite, the two complexes formed with ligand stereoisomers have to present different magnetic behaviors as a function of temperature, which implies that one of them at least exhibits a thermally-induced spin crossover. In the temperature range where the spin states of the two species differ, it becomes possible to induce a spin change of the metal ion by photoisomerizing the ligand.

Using 4-styrylpyridine (stpy) as the *cis–trans* photoisomerizable ligand, we attempted to get complexes of the type $Fe(L)_4(X)_2$ (L being stpy and X^- an anionic ligand), which may undergo a spin conversion or act as precursors in the synthesis of spin-crossover compounds.[4] The first species we obtained[5] complies with the unexpected formula [Fe(*trans*-stpy)$_2$(MeOH)$_2$(NCS)$_2$]·2*trans*-stpy: two of the four styrylpyridine ligands are not bound to the metal ion. In this complex, iron(II) was shown to retain the HS state at any temperature.

The present work is related to the first pair of compounds of the type $Fe(stpy)_4(X)_2$ including the *trans* and *cis* forms of 4-styrylpyridine, respectively. Thiocyanate ions were taken as X^- ligands. Fe(*trans*-stpy)$_4$(NCS)$_2$ (**1**) exhibits a thermally-induced spin change. As expected, Fe(*cis*-stpy)$_4$(NCS)$_2$ (**2**) presents a different spin-state behavior, since it was found to be HS whatever the temperature may be. In this paper, we describe the strategy adopted to change the spin state of the metal ion when photoisomerizing the ligand, and we report the syntheses of compounds **1** and **2**, their X-ray diffraction structures, and their magnetic behaviors as a function of temperature.

* Abstract published in *Advance ACS Abstracts*, April 15, 1994.

(1) (a) Université de Paris-Sud. (b) Université de Bordeaux I.

(2) (a) Gütlich, P. *Struct. Bonding (Berlin)* **1981**, *44*, 83. (b) König, E.; Ritter, G.; Kulshreshtha, S. K. *Chem. Rev.* **1985**, *85*, 219. (c) Rao, C. N. R. *Int. Rev. Phys. Chem.* **1985**, *4*, 19. (d) König, E. *Prog. Inorg. Chem.* **1987**, *35*, 527. (e) Beattie, J. K. *Adv. Inorg. Chem.* **1988**, *32*, 1. (f) Bacci, M. *Coord. Chem. Rev.* **1988**, *86*, 245. (g) Toftlund, H. *Coord. Chem. Rev.* **1989**, *94*, 67. (h) König, E. *Struct. Bonding (Berlin)* **1991**, *76*, 51. (i) Zarembowitch, J. *New J. Chem.* **1992**, *16*, 255.

(3) Gütlich, P.; Hauser, A. *Coord. Chem. Rev.* **1990**, *97*, 1.

(4) Claude, R.; Real, J. A.; Zarembowitch, J.; Kahn, O.; Ouahab, L.; Grandjean, D.; Boukheddaden, K.; Varret, F.; Dworkin, A. *Inorg. Chem.* **1990**, *29*, 4442.

(5) Roux, C.; Zarembowitch, J.; Gallois, B.; Bolte, M. *New J. Chem.* **1992**, *16*, 671.

0020-1669/94/1333-2273$04.50/0

Table 1. Crystal Characteristics and Conditions for Crystallographic Data Collections and Structure Refinements ($T \approx 293$ K)

	Fe(*trans*-stpy)$_4$(NCS)$_2$ (1)	Fe(*cis*-stpy)$_4$(NCS)$_2$ (2)
formula	$C_{54}H_{44}N_6S_2Fe$	$C_{54}H_{44}N_6S_2Fe$
fw	896.51	896.51
cryst system	orthorhombic	monoclinic
space group	$Pna2_1$	$P2_1/n$
Z	4	2
a, Å	32.004(3)	13.115(2)
b, Å	15.394(1)	12.569(3)
c, Å	9.842(1)	14.574(3)
β, deg	90.0	91.90(1)
V, Å^3	4848.9	2401.1
λ, Å	1.541 78 (Cu Kα)	0.710 69 (Mo Kα)
ρ(calcd), g cm^{-3}	1.229	1.240
μ, cm^{-1}	18.19	4.4
R^a	0.044	0.067
$R_w{}^a$	0.043	0.062

^{a} $R = \sum||F_o| - |F_c||/\sum|F_o|$; $R_w = \sum w^{1/2}||F_o| - |F_c||/\sum w^{1/2}|F_o|$.

Experimental Section

Syntheses. ***trans*-4-Styrylpyridine** was obtained by reacting equimolar amounts of 4-methylpyridine and benzaldehyde in acetic anhydride, according to a procedure we recently reported.[5] The resulting compound was in the form of white needles.

Anal. Calcd for $C_{13}H_{11}N$ (M_r = 181.23): C, 86.15; H, 6.12; N, 7.73. Found: C, 86.19; H, 6.22; N, 7.43. ^{1}H NMR data (ppm) in $CDCl_3$: 8.62 (2H); 7.6 (4H); 7.4 (4H); 7.05 (1H). The NMR spectrum characteristics agree with those reported by Hsu et al.[6]

***cis*-4-Styrylpyridine** was prepared by a Wittig reaction, as described by Williams et al.[7] The procedure consisted in treating 4-pyridinecarboxaldehyde with the phosphorus ylide obtained by addition of benzyltriphenylphosphonium chloride to sodium ethanolate. The resulting compound was a colorless liquid.

Boiling point, under a pressure of 0.4 mm of mercury: 103–104 °C. Anal. Found: C, 86.13; H, 6.13; N, 7.80. ^{1}H NMR data (ppm) in CD_3CN: 8.45 (2H); 7.3–7.1 (several peaks, 7H); 6.85 (doublet, 1H); 6.60 (doublet, 1H).

Fe(*trans*-stpy)$_4$(NCS)$_2$ (1) was entirely synthesized under an argon atmosphere. Anhydrous methanol, used as the solvent, was obtained by distillation upon $CaCl_2$ and drying over 3-Å molecular sieves. To a solution of KNCS (131.0 mg, 1.35 mmol) in anhydrous MeOH (9 mL) was added a solution of $FeSO_4 \cdot 7H_2O$ (185.6 mg, 0.67 mmol) in the same solvent (4.5 mL). The mixture was stirred for 10 min, decanted off, and filtered. The precipitate of potassium sulfate was washed with 2 mL of anhydrous MeOH. The methanolic fractions containing $Fe(NCS)_2$ were then collected, and the resulting solution was added dropwise to a suspension of *trans*-4-styrylpyridine (366.4 mg, 2.02 mmol) in MeOH (9 mL) and H_2O (9 mL). A purple-red precipitate formed immediately. The reaction mixture was still stirred for 2 h. The precipitate was separated by filtration and dried under an argon stream.

Anal. Calcd for $C_{54}H_{44}N_6S_2Fe$ (M_r = 896.93): C, 72.31; H, 4.94; N, 9.37; S, 7.15; Fe, 6.23. Found: C, 72.60; H, 4.88, N, 9.03; S, 7.23; Fe, 6.12.

Crystals of **1** were obtained by adding the solution of $Fe(NCS)_2$, prepared as described above, to a solution of *trans*-4-styrylpyridine (366.4 mg, 2.02 mmol) in MeOH (24 mL) and H_2O (9 mL). Slow evaporation of the solvent under an argon stream led to red crystals with rectangular faces.

Anal. Found: C, 72.54; H, 5.18; N, 9.16; S, 6.92; Fe, 5.94.

Fe(*cis*-stpy)$_4$(NCS)$_2$ (2) was prepared in the form of powder or crystals by following the procedures adopted for **1**, *trans*-4-styrylpyridine being then replaced by *cis*-4-styrylpyridine. The powder is yellow. The crystals are orange, with hexagonal faces.

Anal. Found for the powder: C, 71.79; H, 4.69; N, 9.77; S, 7.11; Fe, 6.14. Found for the crystals: C, 72.12; H, 5.05; N, 9.39; S, 7.18; Fe, 6.20.

(6) Hsu, M. T. S.; Rosenberg, M. L.; Parker, J. A.; Heimbuch, A. H. *J. Appl. Polym. Sci.* **1981**, *26*, 1975.
(7) Williams, J. L. R.; Adel, R. E.; Carlson, J. M.; Reynolds, G. A.; Borden, D. G.; Ford, J. A., Jr. *J. Org. Chem.* **1963**, *28*, 387.

Table 2. Fractional Atomic Coordinates (×10^4) and Equivalent Isotropic Thermal Parameters (×10^3 Å^2) for the Non-Hydrogen Atoms of Fe(*trans*-stpy)$_4$(NCS)$_2{}^a$

	x/a	y/b	z/c	$U_{eq}{}^b$
Fe	1150(1)	1317(1)	2500(1)	54(1)
N500	1748(2)	1473(4)	3368(8)	63(8)
C501	2062(3)	1654(5)	3864(9)	56(10)
S502	2508(1)	1897(2)	4535(4)	113(4)
N600	562(2)	1179(4)	1574(9)	76(10)
C601	271(3)	1009(5)	1002(10)	64(11)
S602	−158(1)	824(2)	257(5)	166(5)
N100	1147(2)	2687(4)	1792(7)	52(7)
C101	815(3)	3201(6)	1888(10)	67(11)
C102	802(3)	4053(6)	1407(9)	59(11)
C103	1154(3)	4403(5)	782(9)	57(10)
C104	1499(3)	3867(6)	684(11)	79(13)
C105	1479(3)	3033(6)	1178(11)	68(11)
C106	1178(3)	5295(6)	250(10)	71(11)
C107	879(3)	5865(6)	279(10)	65(10)
C108	901(3)	6761(6)	−315(10)	61(11)
C109	541(3)	7241(7)	−486(11)	81(12)
C110	555(4)	8049(7)	−1080(12)	93(15)
C111	933(5)	8402(7)	−1458(12)	96(15)
C112	1288(4)	7956(8)	−1251(12)	93(15)
C113	1279(3)	7133(7)	−687(12)	84(14)
N200	1108(2)	−71(5)	3077(9)	61(9)
C201	1232(2)	−337(6)	4313(12)	60(12)
C202	1288(3)	−1204(6)	4649(11)	68(12)
C203	1211(3)	−1835(6)	3668(14)	68(14)
C204	1051(3)	−1557(6)	2437(15)	85(15)
C205	1010(3)	−697(6)	2191(10)	78(13)
C206	1294(3)	−2775(7)	3899(15)	93(16)
C207	1474(3)	−3126(8)	4823(16)	96(18)
C208	1599(3)	−4052(7)	5043(16)	82(16)
C209	1731(4)	−4281(8)	6277(16)	104(18)
C210	1838(4)	−5087(10)	6593(15)	115(18)
C211	1833(3)	−5736(7)	5633(17)	90(16)
C212	1720(4)	−5528(8)	4311(17)	110(18)
C213	1599(4)	−4667(8)	4022(15)	109(18)
N300	882(2)	1717(4)	4459(8)	57(7)
C301	551(3)	1318(5)	4997(11)	73(12)
C302	349(3)	1568(6)	6152(13)	79(13)
C303	483(3)	2305(6)	6812(9)	64(11)
C304	837(3)	2713(5)	6325(10)	58(10)
C305	1030(2)	2403(5)	5167(10)	60(10)
C306	234(3)	2660(6)	7929(11)	81(12)
C307	205(3)	3483(6)	8293(10)	76(12)
C308	−70(3)	3867(6)	9286(10)	65(11)
C309	−275(2)	3393(6)	10284(11)	67(11)
C310	−546(3)	3809(7)	11171(11)	85(14)
C311	−610(3)	4704(8)	11043(13)	93(15)
C312	−406(3)	5156(6)	10065(12)	83(13)
C313	−138(3)	4747(6)	9212(11)	74(11)
N400	1480(2)	911(4)	604(9)	56(9)
C401	1355(3)	1138(5)	−624(13)	67(12)
C402	1536(3)	863(5)	−1811(11)	66(12)
C403	1862(3)	265(6)	−1768(12)	55(11)
C404	2001(2)	26(5)	−500(13)	58(11)
C405	1806(3)	354(6)	643(10)	61(11)
C406	2036(3)	−92(6)	−3013(10)	64(12)
C407	2224(2)	−882(6)	−3095(10)	59(10)
C408	2342(2)	−1331(7)	−4356(11)	59(13)
C409	2329(2)	−944(7)	−5650(15)	79(14)
C410	2406(3)	−1421(9)	−6822(12)	94(16)
C411	2510(3)	−2312(9)	−6649(16)	96(18)
C412	2530(3)	−2676(7)	−5423(19)	87(14)
C413	2445(2)	−2186(7)	−4262(11)	68(13)

^{a} Numbers in parentheses are estimated standard deviations in the last significant digit. ^{b} $U_{eq} = {}^1/_3(\sum_i\sum_j a_i^* a_j^* a_i a_j U_{ij})$.

Solution and Refinement of the X-ray Structures. Preliminary X-ray photographic exposures clearly establish that Fe(*cis*-stpy)$_4$(NCS)$_2$ crystals are modified after they have been stored in daylight for several days. The diffraction pattern shows a noticeable broadening of Bragg diffraction peaks and an increase in the diffuse background. This may be correlated with the *cis* → *trans* isomerization of the styrylpyridine ligand, which would result in lattice strain and, hence, in crystal damage.

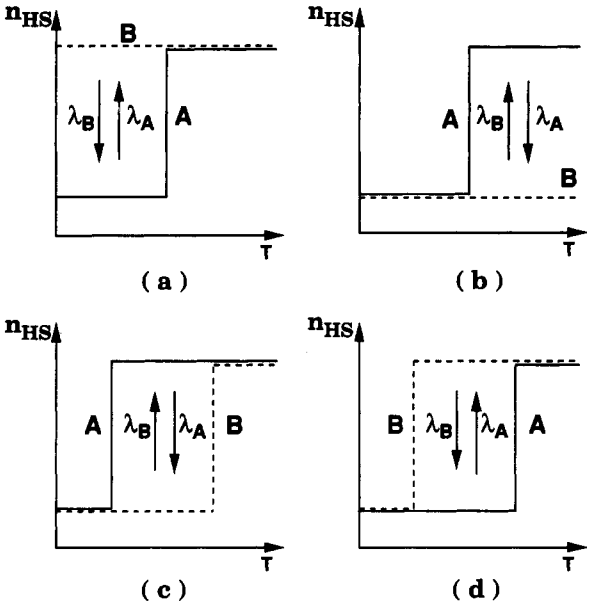

Figure 1. Principle of the method used to obtain ligand-driven light-induced spin change (LD–LISC): n_{HS} = HS form fraction; T = temperature; **A** = spin-crossover complex formed with one of the ligand isomer; **B** = complex formed with the ligand second isomer (see text); λ_A, λ_B = irradiating wavelengths used for **A** → **B** and **B** → **A** conversions, respectively (one of these photoconversions may be replaced by a thermal reversion).

In order to minimize these effects prior to data collections, particular care has been taken in storage conditions (these were performed in complete darkness, at freezing temperature) and in the choice of the mounted crystal.

For both compounds **1** and **2**, intensity data collections were carried out at $T \approx 293$ K, in complete darkness, on an Enraf-Nonius CAD-4 diffractometer, using graphite-monochromatized radiations. The data collection time was limited to 3 days by optimizing the scan speed (1 deg min^{-1}). When measurements were performed, a monitoring of the profiles and intensities of three standard reflections was carried out every 1 h: no noticeable change was observed in the peak widths, and the overall linear intensity decrease did not exceed 0.025. Details of crystal characteristics, data collections, and structure refinements are summarized in Table 1. Lattice parameters were obtained from a least-squares refinement of the setting angles of 25 reflections in the $8 \leq \theta \leq 17°$ (**1**) and $12 \leq \theta \leq 25°$ (**2**) ranges. No significant changes were observed between the values obtained before and after the data collections. The intensities of 2261 (**1**) and 3503 (**2**) independent Bragg reflections ($1 \leq \theta \leq 50°$ (**1**) and $1 \leq \theta \leq 25°$ (**2**)) were gathered by $\omega/2\theta$ scans. Lorentz polarization and absorption corrections were applied. Totals of 1844 (**1**) and 1696 (**2**) reflections for which $F_o > 3\sigma(F_o)$ (**1**) and $F_o > 4\sigma(F_o)$ (**2**) were used to refine the structures.

The complete structures were solved by direct methods.[8,9] The full-matrix refinement, based on F_o, was carried out by using the program SHELX76.[10] Atomic scattering factors were taken from ref 11. Final refinement minimizing $\sum w(|F_o| - |F_c|)^2$ converges to $R = \sum||F_o| - |F_c||/\sum|F_o| = 0.044$, $R_w = \sum w^{1/2}||F_o| - |F_c||/\sum w^{1/2}|F_o| = 0.043$ for **1** and $R = 0.067$, $R_w = 0.062$ for **2**. Non-hydrogen atoms were refined anisotropically. All hydrogen atoms were placed in computed positions and isotropically refined.

Magnetic Measurements. Magnetic susceptibility measurements were performed in the cooling mode for compound **2** and at both decreasing and increasing temperatures (in order to search for the possible existence of a thermal hysteresis effect) for compound **1**, using a Faraday-type magnetometer equipped with an Oxford Instruments helium continuous-flow cryostat. The independence of the susceptibility value with regard to the applied magnetic field was checked for each sample at room temperature. $HgCo(NCS)_4$ was chosen as the susceptibility standard. Diamagnetic corrections were estimated at -510×10^{-6} cm^{-3} mol^{-1}. Temperature was varied at the rate of 1 K min^{-1} in the cooling mode and $\approx$0.5 K min^{-1} in the heating mode. The uncertainty of its value is about 0.1 K.

(8) Sheldrick, G. M. *SHELX86, Program for Structure Determination*: University of Göttingen: Göttingen, FRG, 1986.
(9) Gilmore, C. J. *J. Appl. Crystallogr.* **1984**, *17*, 42.
(10) Sheldrick, G. M. *SHELX76, System of Computing Programs*: University of Cambridge: Cambridge, England, 1976.
(11) *International Tables for X-ray Crystallography*; Kynoch Press: Birmingham, England, 1974; Vol. 4, p 99.

Principle of the Method

The principle of the new method (summarized above) we are developing with a view to obtaining ligand-driven light-induced spin changes (LD–LISC) is schematized in Figure 1. This method can be adapted to any photochemical process capable of modifying the ligand-field strength significantly. The procedure we used is based on the utilization of *cis–trans* photoisomerizable ligands. The first step consists in using one of the ligand isomers to get a transition-metal complex (**A**) that exhibits a thermally-induced spin crossover; the diagrams in Figure 1a–d show this property of **A** in the form of the evolution of the high-spin fraction (n_{HS}) as a function of temperature. It follows that, in this complex, a slight variation of the ligand-field strength should give rise to a change in the magnetic behavior of the metal ion. Consequently, the species **B** formed with the ligand second isomer is expected either to be in the HS state (Figure 1a) or in the LS state (Figure 1b) at any temperature or to exhibit a spin crossover at a temperature higher (Figure 1c) or lower (Figure d) than that of **A**. In each case, there exists a temperature range where ligand photoisomerization should result in a change of the metal ion spin state.

It should be noted that the *trans* → *cis* and *cis* → *trans* transformations of the ligand may be induced either under irradiation at two different wavelengths (as shown in Figure 1) or according to a photochemical process in one direction and a thermal process in the other one.

For the spin change to be detected under the most favorable conditions, compounds **A** and **B** have to meet several requirements: (i) similar geometries of the coordination cores; (ii) spin states different in a rather wide temperature range; (iii) high quantum yields for ligand photoisomerization.

Results

Description of the Structure of 1. Compound **1** crystallizes in the $Pna2_1$ orthorhombic space group ($Z = 4$). Owing to the nonspecial position of the iron atom, the asymmetric unit consists of a Fe(*trans*-stpy)$_4$(NCS)$_2$ molecule. A perspective drawing of this molecule, including the numbering of the non-hydrogen atoms, is given in Figure 2. Fractional atomic coordinates and equivalent isotropic thermal parameters are listed in Table 2.

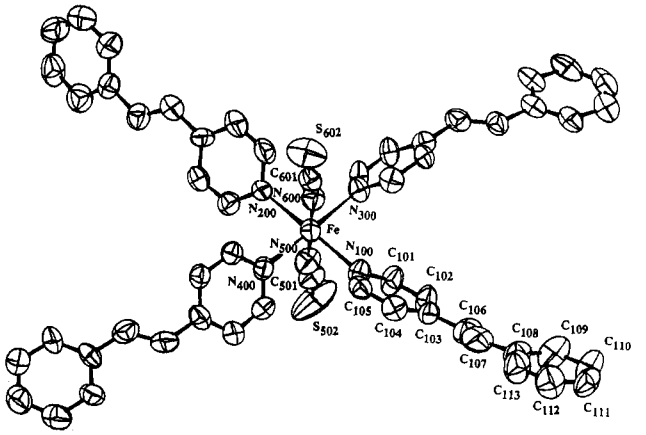

Figure 2. Perspective drawing of the Fe(*trans*-stpy)$_4$(NCS)$_2$ (**1**) molecule including the numbering of non-hydrogen atoms. Hydrogen atoms were omitted for clarity.

Each iron atom is surrounded by six nitrogen atoms belonging to two $(NCS)^-$ groups in a *trans* position and to the pyridine rings

Table 3. Selected Bond Lengths (Å) for Fe(*trans*-stpy)$_4$(NCS)$_2$[a,b]

Fe–N100	2.222(6)	Fe–N200	2.215(7)
Fe–N300	2.198(7)	Fe–N400	2.234(8)
Fe–N500	2.108(7)	Fe–N600	2.103(8)
N500–C501	1.151(11)	N600–C601	1.120(12)
C501–S502	1.617(10)	C601–S602	1.582(10)
N100–C101	1.328(11)	C107–C108	1.499(12)
N100–C105	1.333(12)	C108–C109	1.379(14)
C101–C102	1.394(13)	C108–C113	1.389(14)
C102–C103	1.391(12)	C109–C110	1.375(15)
C103–C104	1.382(12)	C110–C111	1.378(19)
C103–C106	1.473(12)	C111–C112	1.342(19)
C104–C105	1.374(13)	C112–C113	1.383(16)
C106–C107	1.299(12)		

[a] Numbers in parentheses are estimated standard deviations in the least significant digits. [b] Concerning styrylpyridine bond lengths, only the values relative to one of the four ligands (stpy1) are listed. The other data are given as supplementary material.

Table 4. Selected Angles (deg) for Fe(*trans*-stpy)$_4$(NCS)$_2$[a]

N500–Fe–N600	178.1(3)	Fe–N100–C105	121.2(6)
N100–Fe–N500	91.3(3)	Fe–N200–C201	120.5(6)
N100–Fe–N600	87.5(3)	Fe–N200–C205	122.9(7)
N200–Fe–N500	93.6(3)	Fe–N300–C301	122.0(6)
N200–Fe–N600	87.6(3)	Fe–N300–C305	122.3(5)
N300–Fe–N500	88.1(3)	Fe–N400–C401	123.1(6)
N300–Fe–N600	93.4(3)	Fe–N400–C405	121.3(6)
N400–Fe–N500	86.6(3)	C101–N100–C105	115.5(8)
N400–Fe–N600	91.9(3)	C201–N200–C205	116.1(8)
N100–Fe–N200	174.9(3)	C301–N300–C305	115.7(7)
N100–Fe–N300	90.4(2)	C401–N400–C405	115.4(8)
N100–Fe–N400	90.3(3)	C103–C106–C107	125.7(9)
N200–Fe–N300	91.2(3)	C106–C107–C108	125.3(9)
N200–Fe–N400	88.5(3)	C203–C206–C207	129.4(12)
N300–Fe–N400	174.7(2)	C206–C207–C208	131.6(12)
Fe–N500–C501	172.3(6)	C303–C306–C307	126.8(9)
Fe–N600–C601	170.6(7)	C306–C307–C308	128.3(9)
N500–C501–S502	178.8(8)	C403–C406–C407	123.9(9)
N600–C601–S602	175.6(9)	C406–C407–C408	125.8(8)
Fe–N100–C101	123.2(6)		

[a] Numbers in parentheses are estimated standard deviations in the least significant digits.

of the four styrylpyridine ligands, so that coordination is found to establish an [Fe–N_6] octahedron. A selection of interatomic distances and bond angles is given in Tables 3 and 4, respectively.

Whereas the $(NCS)^-$ groups are quasi linear (N500–C501–S502 = 178.8(8)°, N600–C601–S602 = 175.6(9)°), the Fe–N–C(S) linkages are rather bent (Fe–N500–C501 = 172.3(6)°, Fe–N600–C601 = 170.6(7)°). The Fe–N distances involved (Fe–N500 = 2.108(7) Å, Fe–N600 = 2.103(8) Å) are shorter than the Fe–N(stpy) ones (mean value = 2.217 Å), which leads to a distortion of the [Fe–N_6] octahedron. However, this distortion remains limited, as shown by the values, close to 180 or 90°, of the N–Fe–N angles (see Table 4).

All the styrylpyridine moieties are in a *trans*-configuration. Denoting each of them by the first number of the labeling of its atoms and each atom by its last digit, the C3–C6–C7–C8 dihedral angles are actually rather close to 180°:

stpy1: 182.5° stpy2: 186.3°

stpy3: 172.6° stpy4: 169.3°

A further examination of the intramolecular geometry of these ligands reveals differences in their conformations. The values of the angle between the least-square planes defined by the atoms of each ring strongly differ: 11.8° (stpy1); 14.0° (stpy2); 45.5° (stpy3); 36.2° (stpy4).

No evidence of a disorder in the styrylpyridine conformation is revealed from the thermal motion of the atoms. Whatever the considered ligand, the thermal coefficients of the phenyl ring atoms do not drastically differ from those of the pyridine ring.

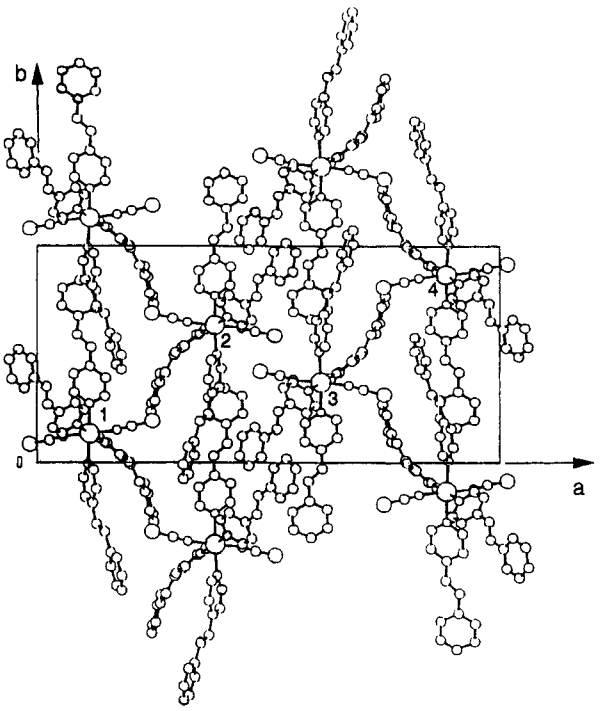

Figure 3. Projection of the crystal structure of Fe(*trans*-stpy)$_4$(NCS)$_2$ (**1**) along the *c* axis. Key: (1) x, y, z; (2) $^1/_2 - x, ^1/_2 + y, ^1/_2 + z$; (3) $^1/_2 + x, ^1/_2 - y, z$; (4) $1 - x, 1 - y, ^1/_2 + z$.

Table 5. Intermolecular Distances (Å) Shorter Than the Sum of the van der Waals Distances in Fe(*trans*-stpy)$_4$(NCS)$_2$[a]

sym operation	associated transl	atoms involved	dists
$-x, -y, ^1/_2 + z$		C301···S602	3.538(5)
		C310···C207	3.418(6)
		C310···C208	3.567(7)
		C311···C208	3.463(6)
$^1/_2 - x, ^1/_2 + y, ^1/_2 + z$		C105···C413	3.488(6)
x, y, z	001	C202···C408	3.517(7)
		C202···C409	3.368(6)
		C207···C412	3.458(6)
		C207···C413	3.542(7)
		C308···C102	3.498(7)
x, y, z	00$\bar{1}$	C102···C308	3.498(7)
		C408···C202	3.517(7)
		C409···C202	3.368(6)
		C412···C207	3.458(6)
		C413···C207	3.542(7)
$-x, -y, ^1/_2 + z$	00$\bar{1}$	C207···C310	3.418(6)
		C208···C310	3.567(7)
		C208···C311	3.463(6)
		S602···C301	3.538(5)
$^1/_2 - x, ^1/_2 + y, ^1/_2 + z$	00$\bar{2}$	C410···C210	3.536(6)
$^1/_2 - x, ^1/_2 + y, ^1/_2 + z$	0$\bar{1}$1	C210···C410	3.536(6)
$^1/_2 - x, ^1/_2 + y, ^1/_2 + z$	0$\bar{1}\bar{1}$	C413···C105	3.488(6)

[a] The first mentioned atom is related to a given central x, y, z molecule.

The ratio between the relative U_{eq} mean values does not exceed 1.4. This result seems to indicate that the *trans*-configuration is stable: a significant amount of the *cis*-configuration would give rise to some disorder in the phenyl moiety (vide infra). The slightly larger U_{eq} values of the atoms of this ring are consistent with the fact that these atoms are in the outshell of the molecule and, hence, are less constrained by intramolecular steric effects than those of the pyridine ring.

Figure 3 shows a projection of the structure along the *c* axis. Parallel to the *a* direction, the iron atoms alternate at the coordinates $z = 0.25$ and $z = 0.75$. In the *bc* plane, molecules correspond to each other by translation. The crystal cohesion is mainly acheived by van der Waals interactions between the styrylpyridine ligands of adjacent molecules. It does not involve any significant π contribution, since none of these ligands is parallel

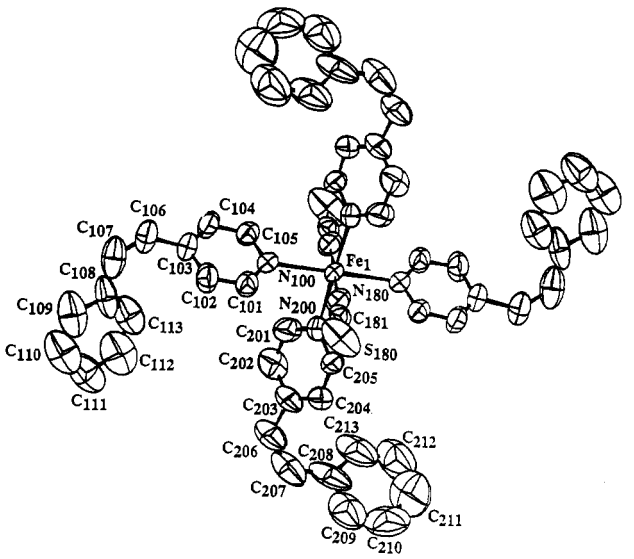

Figure 4. Perspective drawing of the Fe(*cis*-stpy)$_4$(NCS)$_2$ (**2**) molecule including the numbering of non-hydrogen atoms. Hydrogen atoms were omitted for clarity.

Table 6. Fractional Atomic Coordinates (×10^4) and Equivalent Isotropic Thermal Parameters (×10^3 Å^2) for the Non-Hydrogen Atoms of Fe(*cis*-stpy)$_4$(NCS)$_2$[a]

	x/a	*y/b*	*z/c*	U_{eq}[b]
Fe	5000(1)	0(1)	0(1)	54(1)
N180	4604(4)	264(5)	−1369(4)	74(2)
C181	4408(4)	433(5)	−2135(5)	66(2)
S180	4149(2)	678(3)	−3202(2)	140(2)
N100	6432(4)	976(4)	−128(4)	71(2)
C101	6834(5)	1141(6)	−942(5)	84(2)
C102	7669(5)	1792(6)	−1065(5)	94(2)
C103	8120(5)	2297(5)	−302(5)	76(2)
C104	7717(5)	2125(6)	519(5)	82(2)
C105	6899(5)	1451(6)	597(5)	73(2)
C106	8948(5)	3080(7)	−409(5)	105(2)
C107	9797(6)	3019(7)	−838(5)	122(2)
C108	10268(5)	2122(6)	−1263(5)	120(2)
C109	11014(5)	2376(6)	−1885(5)	151(2)
C110	11523(6)	1534(6)	−2291(6)	161(2)
C111	11314(6)	473(6)	−2101(6)	171(2)
C112	10607(6)	266(6)	−1428(6)	173(2)
C113	10071(6)	1075(6)	−1003(5)	141(2)
N200	4073(4)	1421(4)	405(4)	66(2)
C201	3153(5)	1591(6)	13(5)	92(2)
C202	2503(6)	2375(7)	287(5)	106(2)
C203	2780(5)	3059(6)	983(5)	83(2)
C204	3738(5)	2903(5)	1388(5)	76(2)
C205	4339(5)	2077(5)	1086(5)	66(2)
C206	2036(6)	3843(7)	1313(6)	117(2)
C207	2210(7)	4803(7)	1635(6)	134(2)
C208	3110(6)	5437(6)	1594(5)	148(2)
C209	3438(6)	6045(7)	2349(6)	176(2)
C210	4312(6)	6679(7)	2374(6)	199(2)
C211	4870(7)	6675(8)	1576(6)	232(2)
C212	4559(7)	6164(8)	764(6)	214(2)
C213	3726(6)	5483(6)	834(5)	186(2)

[a] Numbers in parentheses are estimated standard deviations in the last significant digit. [b] $U_{eq} = {}^1/_3(\sum_i\sum_j a_i^* a_j^* a_i a_j U_{ij})$.

to another one. Atoms of the (NCS)$^-$ groups are just slightly involved in the molecular packing. Only one S···C contact is observed, as shown in Table 5 which gives the intermolecular distances shorter than the sum of the atomic van der Waals radii.

Description of the Structure of 2. Compound **2** crystallizes in the monoclinic $P2_1/n$ space group. The unit cell contains two Fe(*cis*-stpy)$_4$(NCS)$_2$ molecules. Figure 4 shows a perspective drawing of one of them, together with the numbering of the atoms of the asymmetrical unit: the iron atom is on the inversion center, and the asymmetrical unit consists of two styrylpyridine ligands,

Table 7. Selected Bond Lengths (Å) for Fe(*cis*-stpy)$_4$(NCS)$_2$[a,b]

Fe–N100	2.256(5)	Fe–N180	2.072(6)
Fe–N200	2.251(5)	N180–C181	1.156(9)
		C181–S180	1.611(8)
N100–C101	1.331(9)	C107–C108	1.435(11)
N100–C105	1.344(9)	C108–C109	1.392(10)
C101–C102	1.384(10)	C108–C113	1.397(11)
C102–C103	1.395(10)	C109–C110	1.394(11)
C103–C104	1.340(10)	C110–C111	1.391(11)
C103–C106	1.478(10)	C111–C112	1.396(11)
C104–C105	1.375(9)	C112–C113	1.393(11)
C106–C107	1.299(11)		

[a] Numbers in parentheses are estimated standard deviations in the least significant digits. [b] Concerning styrylpyridine bond lengths, only the values relative to stpy1 are listed. The data relative to stpy2 are given as supplementary material. The corresponding distances, in the two ligand conformations, do not differ by more than 0.044 Å.

Table 8. Selected Angles (deg) for Fe(*cis*-stpy)$_4$(NCS)$_2$[a]

N100–Fe–N200	92.8(2)	Fe–N100–C101	120.9(4)
N100–Fe–N180	90.9(2)	Fe–N100–C105	122.4(4)
N200–Fe–N180	90.3(2)	Fe–N200–C201	120.2(5)
Fe–N180–C181	177.9(5)	Fe–N200–C205	123.9(4)
N180–C181–S180	179.2(6)		
C101–N100–C105	116.7(6)	C201–N200–C205	115.6(6)
C102–C103–C106	120.8(6)	C202–C203–C206	119.8(7)
C104–C103–C106	120.9(6)	C204–C203–C206	123.7(7)
C103–C106–C107	131.0(7)	C203–C206–C207	128.4(8)
C106–C107–C108	130.0(8)	C206–C207–C208	129.2(8)
C107–C108–C109	115.0(6)	C207–C208–C209	120.5(7)
C107–C108–C113	122.5(7)	C207–C208–C213	124.0(7)

[a] Numbers in parentheses are estimated standard deviations in the least significant digit.

labeled stpy1 and stpy2, and one (NCS)$^-$ group. Fractional atomic coordinates and equivalent isotropic thermal parameters are given in Table 6. Selected bond lengths and bond angles are listed in Tables 7 and 8, respectively. Both styrylpyridine ligands are in the *cis*-configuration but have different conformations. Ligand stpy1 is in a gauche minus conformation (dihedral angles C102–C103–C106–C107 = −51.9° and C103–C106–C107–C108 = −8.3°). The plane of the pyridine moiety is oriented at 66.7° with respect to the plane defined by Fe, N100 and N200, and at 60.3° with respect to the phenyl ring. Ligand stpy2 is in a gauche plus conformation (dihedral angles C202–C203–C206–C207 = 38.3° and C203–C206–C207–C208 = 13.7°). Its pyridine moiety makes an angle of 48.9° with the plane defined by the Fe, N100 and N200 atoms, and an angle of 61.3° with the phenyl ring.

The atoms of the phenyl moiety of both *cis*-styrylpyridine ligands exhibit thermal coefficients which are 2 or 3 times larger than those of the other carbon atoms. This disorder is likely to be not only of dynamic origin (resulting from thermal motions) but also of static origin. As mentioned above, the complex is not stable under daylight exposure at room temperature. Even when the *cis* → *trans* isomerization of styrylpyridine takes place slowly, it is expected to induce a lattice static disorder of the first kind, which should be responsible for the high values of the temperature factors.

The (NCS)$^-$ group is linear (N180–C181–S180 = 179.2°), as well as the Fe–N–C(S) linkage (Fe–N180–C181 = 177.9°). Moreover, the [Fe–N_6] octahedron is almost regular, since all the N–Fe–N angles are close to 90 or 180° (see Table 8); the main distortion comes from the difference between Fe–N(CS) and Fe–N(stpy) bond lengths, which are found to be 2.07 and 2.25 Å, respectively.

A projection of the structure along the *a* axis is shown in Figure 5. The crystal cohesion is achieved by van des Waals interactions. Only few interatomic contacts between neighboring molecules are observed:

$$-{}^1/_2 + x, {}^1/_2 - y, -{}^1/_2 + z \rightarrow \text{S180···C106} = 3.579(13)\ \text{Å}$$

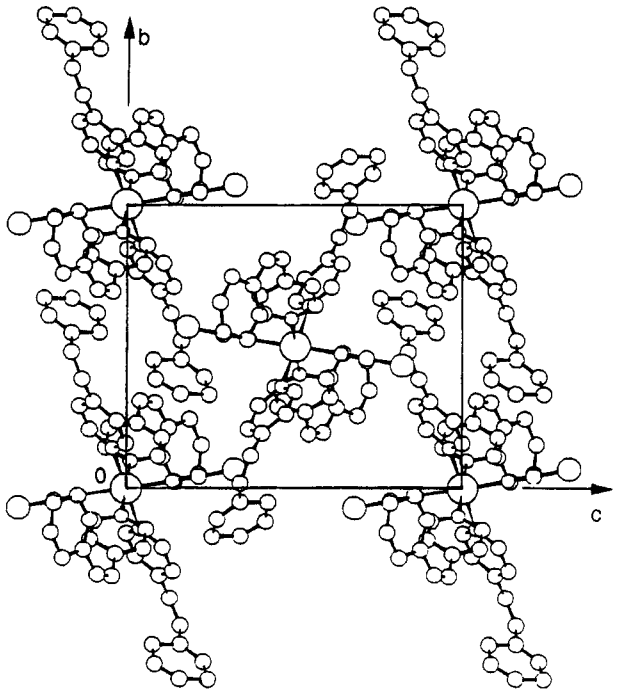

Figure 5. Projection of the crystal structure of Fe(*cis*-stpy)$_4$(NCS)$_2$ (**2**) along the *a* axis.

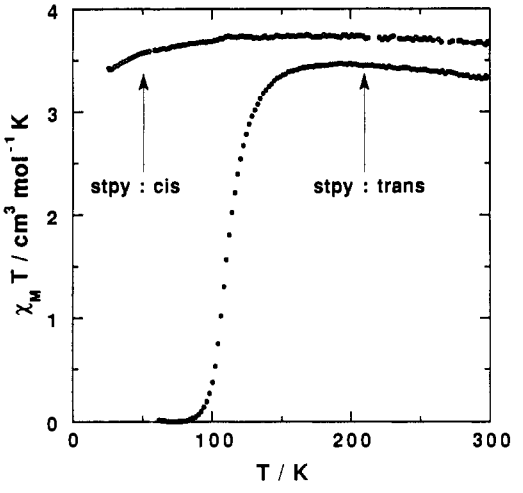

Figure 6. Temperature dependence of $\chi_M T$ for the Fe(stpy)$_4$(NCS)$_2$ compounds formed with *trans*-stpy (full circles) and *cis*-stpy (open circles).

$$-^1/_2 + x, {}^1/_2 - y, {}^1/_2 + z \rightarrow \text{C210}\cdots\text{C112} = 3.345(12)\ \text{Å}$$

$$-x, -y, -z \rightarrow \text{C106}\cdots\text{C207} = 3.535(12)\ \text{Å}$$

$$-x, -y, -z \rightarrow \text{C209}\cdots\text{C102} = 3.550(13)\ \text{Å}$$

Magnetic Properties. The temperature dependence of $\chi_M T$ (χ_M = molar magnetic susceptibility, T = temperature) relative to compounds **1** and **2** is shown in Figure 6.

For **1**, the $\chi_M T$ value at room temperature is 3.33 cm^3 mol^{-1} K, which corresponds to an effective magnetic moment μ_{eff} = 5.16 μ_B. On cooling, this value slightly increases to 3.45 cm^3 mol^{-1} K (μ_{eff} = 5.25 μ_B) at ~185 K and further decreases, first slowly and then rapidly from ~145 K. Below ~60 K, $\chi_M T$ remains constant at 0.04 cm^3 mol^{-1} K (μ_{eff} = 0.57 μ_B). These results provide evidence for a $S = 2 \leftrightarrow S = 0$ spin crossover, centered at ~108 K. Around this temperature, ~65% of the spin change occurs within an interval of 20 K, which is indicative of a moderate cooperativity of the phenomenon. This cooperativity may result, at least partly, from the large number of intermolecular contacts detected in the structure of **1** (see Table 5). The residual HS fraction at low temperature can be estimated at ~1%. It should be noted that no noticeable hysteresis effect can be observed when the $\chi_M T$ vs T curves obtained in the cooling and the warming modes are drawn on the same graph.

For **2**, the $\chi_M T$ product first retains a nearly constant value on cooling, passing from 3.67 cm^3 mol^{-1} K (μ_{eff} = 5.42 μ_B) at room temperature to 3.74 cm^3 mol^{-1} K (μ_{eff} = 5.47 μ_B) at 110 K, and then it decreases slowly. At 30 K it is equal to 3.45 cm^3 mol^{-1} K (μ_{eff} = 5.25 μ_B). This magnetic behavior is typical of a compound in which iron(II) ions are in the HS state.

Discussion

The molecular structures of **1** and **2** show that both compounds have similar pseudo-octahedral coordination cores. The nitrogen atoms of the two (NCS)$^-$ groups are in *trans* position, and those of the four 4-styrylpyridine moieties are nearly coplanar. Moreover, the corresponding metal-ligand distances of the two complexes are close to each other, the mean values relative to Fe–N(CS) being 2.108 and 2.078 Å and those relative to Fe–N(stpy) being 2.21 and 2.25 Å for **1** and **2**, respectively. It follows that the first condition required for **1** and **2** (cf. condition i in Principle of the Method), i.e. similar geometries of the coordination cores, is fulfilled. Moreover, the volumes occupied by one molecule in the crystal are found to be of the same order of magnitude for **1** (1212 Å^3) and **2** (1201 Å^3).

It should be noted that the above-mentioned mean distances compare with those found for Fe–N(CS) and Fe–N(L) bonds (L = heterocyclic ligand) in analogous compounds, viz. Fe(py)$_4$(NCS)$_2$ (2.106 and 2.250 Å),[4] [Fe(py)$_2$(bpym)(NCS)$_2$]·0.25py (2.107, 2.235 Å for Fe–N(py) and 2.218 Å for Fe–N(bpym)),[4] [Fe(py)$_2$(phen)(NCS)$_2$]·0.5py (2.087, 2.214 Å for Fe–N(py) and 2.195 Å for Fe–N(phen)),[12] Fe(phen)$_2$(NCS)$_2$ (2.057 and 2.206 Å),[13] Fe(bpy)$_2$(NCS)$_2$ (2.053 and 2.174 Å),[14] Fe(btz)$_2$(NCS)$_2$ (2.064 and 2.171 Å),[15] and [Fe(btr)$_2$(NCS)$_2$]·H$_2$O (2.098 and 2.135 Å);[16] for the abbreviations, see ref 17. All these species, but the first one, exhibit a spin crossover. Only in Fe(py)$_4$(NCS)$_2$ and [Fe(btr)$_2$(NCS)$_2$]·H$_2$O, where the organic moiety behaves as a monodentate or a bis-monodentate ligand, respectively, are the (NCS)$^-$ groups in a *trans* position, as they are in **1** and **2**.

Regarding the magnetic properties of **1** and **2**, they clearly show that, as wanted (cf. condition ii in Principle of the Method), there exists a temperature range, below ≈90 K, where the spin states of the two compounds are not the same: **1** exhibits a spin crossover centered around 108 K, while **2** retains the HS state at any temperature (see Figure 6).

This difference in magnetic behavior may be accounted for by the fact that *trans*-stpy is a stronger ligand than *cis*-stpy. Actually, the σ-donor character of the two stereoisomers is likely to be of the same order of magnitude. This is suggested, for instance, by the close values of the stability constants of the complexes formed by *trans*- and *cis*-4-styrylpyridine with iodine, which mainly involve a (σ–π^*)-type binding (278 and 265 mol^{-1} L, respectively, at 25° C in *n*-hexane).[18,19] On the other hand, *trans*-stpy is expected to be a better π-acceptor than *cis*-stpy, as shown by the following data, which are indicative of a higher conjugation in

(12) Gallois, B.; Real, J.-A.; Zarembowitch, J. To be published.
(13) Gallois, B.; Real, J.-A.; Hauw, C.; Zarembowitch, J. *Inorg. Chem.* **1990**, *29*, 1152.
(14) Konno, M.; Mikami-Kido M. *Bull. Chem. Soc. Jpn.* **1991**, *64*, 339.
(15) Real, J.-A.; Gallois, B.; Granier, T.; Suez-Panama, F.; Zarembowitch, J. *Inorg. Chem.* **1992**, *31*, 4972.
(16) Vreugdenhil, W.; Van Diemen, J. H.; De Graaf, R. A. G.; Haasnoot, J. G.; Reedijk, J.; Van der Kraan, A. M.; Kahn, O.; Zarembowitch, J. *Polyhedron* **1990**, *9*, 2971.
(17) Abbreviations: py, pyridine; bpym, 2,2′-bipyrimidine; phen, 1,10-phenanthroline; bpy, 2,2′-bipyridine; btz, 2,2′-bi-4,5-dihydrothiazine; btr, 4,4′-bis-1,2,4-triazole.
(18) Aloisi, G.; Cauzzo, G.; Giacometti, G.; Mazzucato, U. *Trans. Faraday Soc.* **1965**, *61*, 1406.
(19) Mazzuccato, U.; Aloisi, G.; Cauzzo, G. *Trans. Faraday Soc.* **1966**, *62*, 2685.

the former molecule: (i) in the same solvent, at room temperature, the $\pi-\pi^*$ absorption band of the *trans* isomer is shifted toward higher wavenumbers with regard to that of the *cis* isomer (λ_{max} = 307 and 279 nm, respectively, in MeOH).[5,20] (ii) in the ^1H NMR spectrum of the two species, the position of the peak corresponding to the protons in ortho-position with regard to the pyridine ring nitrogen atom was found at 8.62 ppm for the *trans* isomer and 8.45 ppm for the *cis* isomer (in $CDCl_3$), which provides evidence for a larger shielding in the latter case. The lower resonance found in *cis*-stpy has to be correlated with the fact that the molecule deviates strongly from planarity, as a consequence of the steric hindrance arising from the proximity of the pyridine and phenyl rings. The structures of **1** and **2** show effectively that this deviation is more important when the ligand is in the *cis*-configuration.

According to the foregoing, compounds **1** and **2** prove to present the magnetic and structural properties required for the LD–LISC effect to be observed. However, Figure 6 shows that the highest temperature at which this observation might be done is ≈90 K. Now, at such a temperature, the cellulose acetate films in which **1** and **2** need to be embedded, in order that the ligand *trans–cis* photoisomerization occurs properly in the solid state, should be quite rigid. The photoisomerization quantum yields $\Phi_{trans\rightarrow cis}$ and $\Phi_{cis\rightarrow trans}$ are then expected to be very low. A similar situation was reported for 4-styrylpyridine in solution: $\Phi_{trans\rightarrow cis}$ was found to vary from 0.37 to 0.46 (with λ_{exc} = 313 nm) at room temperature, according to the nature of the solvent,[5,21-25] while it was shown to be 0 at 77 K, in 3-methylpentane,[24] due to the rigidity of the solvent.

In order to increase the transition temperature of the spin-crossover, and hence the values of $\Phi_{trans\rightarrow cis}$ and $\Phi_{cis\rightarrow trans}$, we are now synthesizing new FeL_4X_2 complexes, where L is either 4-styrylpyridine or a substituted derivative and X^- is varied.

Supplementary Material Available: A full presentation of crystallographic data and experimental parameters for Fe(*trans*-stpy)$_4$(NCS)$_2$ (**1**) and Fe(*cis*-stpy)$_4$(NCS)$_2$ (**2**) (Table S1), fractional positions and isotropic thermal parameters for the hydrogen atoms of **1** (Table S2) and **2** (Table S3), anisotropic thermal parameters for the non-hydrogen atoms of **1** (Table S4) and **2** (Table S5), and distance and angle data for **1** (Tables S6 and S7, respectively) and **2** (Tables S8 and S9, respectively) (9 pages). Ordering information is given on any current masthead page.

(20) (a) Roux, C. Thesis. Université de Paris-Sud (Orsay), 1992. (b) Hamed, M. M.; Aber-Eittah, R. H.; Mohamed, A. A. *J. Chem. Soc.* **1992**, *88*, 955.

(21) Bortolus, P.; Cauzzo, G.; Mazzucato, U. *Z. Phys. Chem. Neue Folge* **1966**, *51*, 264.

(22) Bortolus, P.; Cauzzo, G.; Mazzucato, U.; Galiazzo, G. *Z. Phys. Chem. (Frankfurt am Main)* **1969**, *63*, 29.

(23) Whitten, D. G.; McCall, M. T. *J. Am. Chem. Soc.* **1969**, *91*, 5097.

(24) Bartocci, G.; Mazzucato, U.; Masetti, F.; Galiazzo, G. *J. Phys. Chem.* **1980**, *84*, 847.

(25) Bartocci, G.; Mazzucato, U. *J. Lumin.* **1982**, *27*, 163.